APPLIED SCIENCES AND ENGINEERING

Selective methylation of toluene using CO_2 and H_2 to *para*-xylene

Jiachang Zuo, Weikun Chen, Jia Liu, Xinping Duan, Linmin Ye, Youzhu Yuan*

Toluene methylation with methanol to produce xylene has been widely investigated. A simultaneous side reaction of methanol-to-olefin over zeolites is hard to avoid, resulting in an unsatisfactory methylation efficiency. Here, CO_2 and H_2 replace methanol in toluene methylation over a class of $ZnZrO_x$–ZSM-5 (ZZO-Z5) dual-functional catalysts. Results demonstrate that the reactive methylation species (H_3CO*; * represents a surface species) are generated more easily by CO_2 hydrogenation than by methanol dehydrogenation. Catalytic performance tests on a fixed-bed reactor show that 92.4% xylene selectivity in CO-free products and 70.8% *para*-xylene selectivity in xylene are obtained on each optimized catalyst. Isotope effects of H_2/D_2 and $CO_2/^{13}CO_2$ indicate that xylene product is substantially generated from toluene methylation rather than disproportionation. A mechanism involving generation of reactive methylation species on ZZO by CO_2 hydrogenation and migration of the methylation species to Z5 pore for the toluene methylation to form xylene is proposed.

INTRODUCTION

Para-xylene (PX), as a substantial value-added chemical feedstock, is in great demand with the rapid development of the downstream polyester industry (*1*, *2*). Toluene methylation, an atomic economy process to synthesize PX, has attracted sustained interest in the last decades, and methanol has been widely researched to methylate toluene over zeolite catalysts in a cost-effective manner. However, the temperature of methanol-to-olefin (MTO) side reaction (typically at 400° to 500°C) is approximate to that of toluene/methanol methylation reaction (420° to 480°C) as well over zeolites, leading to the generation of unwanted gaseous hydrocarbon by-products (*3*–*5*). To restrain the side reactions, researchers modified zeolites with the oxides of Mg, P, Si, and so on (*6*–*8*) or performed the reaction at a high toluene/methanol molar ratio of 4:6, causing limited conversion of toluene. Furthermore, the intermediate species of MTO side reaction are prone to be transformed into coke and deposited onto the surface of zeolites, causing rapid deactivation (*9*, *10*). Researchers usually add adequate amount of water to the reactants to retard the deactivation of catalyst (*8*). However, this leads to suppressing the methylation reaction of toluene and increasing the difficulty of industrial production. Once methanol is used as a methylation reagent over zeolites at approximately 450°C, MTO side reaction products are unavoidable and will decrease methanol usage for methylation. Therefore, new types of methylation reagents and catalysts that can work at a relative low temperature must be developed to avoid competing reactions.

The rate-determining step of toluene/methanol methylation is to overcome the high-energy barrier of converting methanol to surface methoxy species. An efficient methylation regent must rapidly generate surface methoxy. In recent years, syngas is used to methylate toluene over Cr_2O_3/ZnO and ZSM-5 (Z5) mixture catalyst (*11*). However, using greenhouse gaseous CO_2 combined with renewable H_2 as methyl source and nontoxic catalyst could be a better avenue. Recently, several types of oxide solid solution catalysts, such as $ZnZrO_x$ (ZZO), $InZrO_x$, $ZnAlO_x$, and $ZnGaO_x$, have been investigated in CO_2 hydrogenated to methanol, olefins, or aromatics via the formate route with the methoxy intermediate (H_3CO*) (*12*–*18*). In tandem catalysts composed of oxides and zeolites, intermediates can migrate between the two components (*19*–*24*). Hydrogenation of CO_2 or CO can also directly produce aromatics (*14*–*16*, *22*, *25*, *26*), but the production distribution is complex and the selectivity to xylene is usually less than 30%. On the basis of the cognizance above, CO_2 and H_2 are introduced as methylation reagents into toluene methylation reaction over ZZO-Z5 dual-functional catalysts. Multiple side reactions that may occur simultaneously need to be suppressed when CO_2 and H_2 are used in toluene methylation, such as xylene isomerization, toluene disproportionation, excessive methylation, and reversed water-gas shift reaction. Therefore, it is highly demanded to design a catalyst that can suppress the impacts of these side reactions as far as possible. In this research, zeolites are modified to inhibit xylene isomerization and toluene disproportionation. The reaction rates of CO_2 hydrogenation and toluene methylation are adapted to suppress excessive methylation. The reaction temperature is reduced as possible to inhibit water-gas shift reaction, which is considered as an endothermic process.

The research highlights the potential for using alternative C1 synthetic unit, greenhouse gaseous CO_2, associated with toluene more efficiently than conventional methanol, as a alternative avenue to synthesize featured xylene. Results show that a 70.8% selectivity to PX in xylene via CO_2 route over the optimized dual-functional ZZO-Z5 while only 32.7% to PX via methanol route over the optimized Z5 can be obtained (Fig. 1). As far as we are aware, there are no reports hitherto on the selective toluene methylation using CO_2 and H_2 to PX.

RESULTS AND DISCUSSION

Initially, the reaction temperature and zeolite Si/Al ratio of dual-functional ZZO-Z5 catalyst were optimized, and then 360°C and a Si/Al ratio of 85 were chosen in the following investigations (fig. S1). Notably, 1,2,4-trimethylbenzen is the main by-product in outlet, but no any 1,2,3- and 1,3,5-trimethylbenzen are detected. Thus, the

State Key Lab of Physical Chemistry of Solid Surfaces, National Engineering Lab for Green Chemical Productions of Alcohols-Ethers-Esters, Collaborative Innovation Center of Chemistry for Energy Materials, College of Chemistry and Chemical Engineering, Xiamen University, Xiamen 361005, P. R. China.
*Corresponding author. Email: yzyuan@xmu.edu.cn

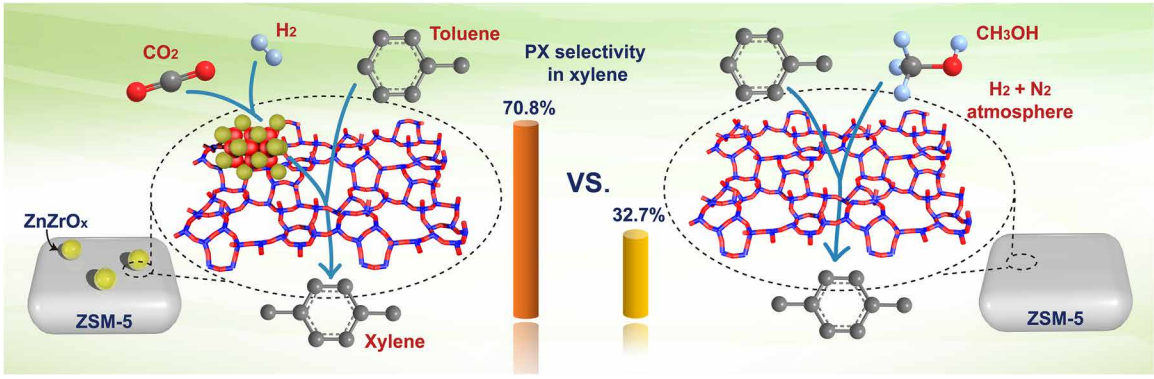

Fig. 1. Toluene methylation using CO_2 and H_2 over optimized dual-functional ZZO-Z5 catalyst versus toluene methylation using methanol over optimized Z5.

deep-methylation reaction of PX and excessive pore size of zeolites lead to the generation of 1,2,4-trimethylbenzen. The mass ratio of ZZO to zeolites was decreased to reduce CO_2 hydrogenation reaction rates and inhibit the deep-methylation reaction. Tetraethyl orthosilicate was deposited on Z5 twice (the modified zeolite was labeled as 2SZ5; 2 represents the time of modification) to minify the pore size of zeolites. Results show that xylene selectivity rises from 66.3 to 92.4%, with the ZZO mass percent decreased to 10% (Fig. 2A). At the same time, 4-ethyltoluene, a deep-methylation by-product with a smaller molecular diameter than 1,2,4-trimethylbenzen, increases compared with the result by unmodified Z5. This result indicates that the pore size of zeolites is effectively decreased, which conforms to the pore width distribution results in Fig. 3F. Controlled experiments that only toluene/N_2 flowed over zeolites were executed to eliminate the influence of toluene disproportionation side reaction. The results show that toluene conversions are only 0.2 and 0.5% for the Z5 and 2SZ5 catalysts, respectively, which indicate that toluene methylation reaction rather than toluene disproportionation is the dominant process that produces xylene.

Although xylene selectivity is improved to more than 90% by adjusting the molar ratio of ZZO and 2SZ5 components in the dual-functional catalyst, the selectivity to PX in xylene is unsatisfied and tends to the thermodynamic equilibrium distribution state (fig. S2A). Moreover, increasing amount of ZZO benefits the CO_2 conversion but leads to the increase of CO selectivity (CO usage, labeled as U_{CO}) and the decrease of methylation selectivity (methylation usage, labeled as U_{methy}) (fig. S2B). In general, blocking active sites on the external surface of zeolites could limit secondary isomerization to increase the PX selectivity in xylene. Hence, the number of times to modify Z5 with TEOS is increased. The selectivity to PX in xylene rises up to 70.8% when zeolites are modified for four times but decreases at five times (Fig. 2B and fig. S3), probably because PX is difficult to migrate and desorb on the modified zeolite surface. Total C1-C5 hydrocarbon selectivity in products without CO is below 0.7% for all dual-functional catalysts, which is superior to that of the methanol route at 400° to 500°C. In addition, the selectivity to PX in xylene could be increased to a high level by carefully designing zeolites. To assess the impact of aromatics directly produced from CO_2 through hydrocarbon pool mechanism, CO_2 + H_2 were inlet over ZZO-4SZ5 catalyst. Results show that the yield of C_{8+} is only 11.6% of that in the C_7H_8 + CO_2 + H_2 route. Moreover, in the presence of toluene, the one-step methylation of toluene with methoxy should be easier to perform than the multistep hydrocarbon pool reaction in the CO_2 + H_2 route. Therefore, we consider that the aromatics directly produced from CO_2 are not dominant in the C_7H_8 + CO_2 + H_2 route.

The methylation of toluene with methanol is normally carried out under ambient pressure. To meaningfully compare the two methylation routes, after screening the effects of different parameters (temperature, pressure, carrier gas, and CH_3OH/C_7H_8 ratio) on the methylation of toluene with methanol over Z5 (fig. S4), we adjust the molar ratio of CH_3OH to C_7H_8 to get a 13.2% toluene conversion close to that in CO_2 route (fig. S4C). Under the same reaction conditions and similar toluene conversion, the differences of CO_2 and methanol routes are investigated, as shown in Fig. 2C. When the unmodified Z5 and ZZO-Z5 are used in methanol and CO_2 routes, respectively, the values of U_{methy} are similar to each other, but the selectivity to C1-C5 (carbon usage for C1-C5, labeled as $U_{C1\text{-}C5}$) is 13.3% in methanol route while only 3.1% to that in CO_2 route. When Z5 is replaced by the modified zeolite 4SZ5, the value of U_{methy} decreases and that of $U_{C1\text{-}C5}$ increases in methanol route, but these data are insignificantly changed in CO_2 route with ZZO-4SZ5 (Fig. 2C). It is certain that the toluene methylation is inhibited but the methanol-to-hydrocarbon (MTH) reaction is enhanced in methanol route due to the decrease in total acid sites of 4SZ5; thereby, the methanol not involved in the methylation reaction is more likely to produce gaseous hydrocarbons or other by-products (fig. S4D). The findings imply that no large amounts of active methylation species are accumulated, and the generated active methylation species can be dynamically consumed in the process of subsequent methylation reaction in CO_2 route. Thereby, the PX selectivity in xylene reaches to 70.8% over ZZO-4SZ5 in CO_2 route, while only 32.7% over 4SZ5 in methanol route. The experimental results proved that the large amounts of active methylation species could participate in deep methylation in methanol route, converting PX to 4-ethyltoluene (represented as C9+ in fig. S4D). Furthermore, the apparent activation energy of methylation estimated by the toluene conversion is approximately 83.2 ± 1.5 kJ mol^{-1} via CO_2 route, which is lower than 108.5 ± 3.6 kJ mol^{-1} of methanol route (Fig. 2D). The results indicate that the active methylation species are easier to generate by CO_2 hydrogenation, and the species can be dynamically reacted by the subsequent methylation step, inhibiting deep-methylation and MTH reactions.

The ZZO-Z5 catalysts were characterized by several methods to indicate the relationship between PX selectivity and physiochemical properties of dual-functional catalysts. Transmission electron microscopy (TEM) and scanning electron microscopy (SEM) images

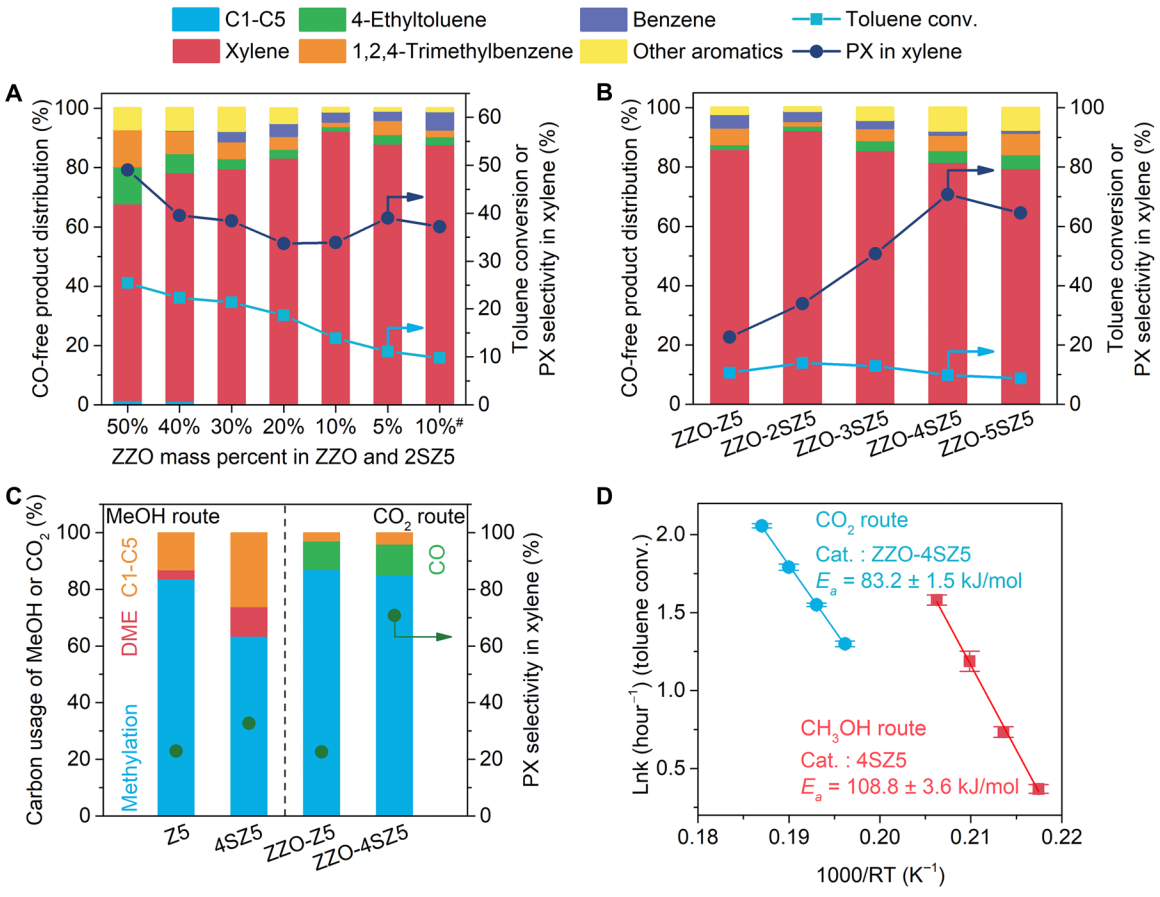

Fig. 2. Catalytic performance of toluene methylation using CO_2+ H_2 or methanol. (**A**) Influence of the ZZO mass percent in ZZO and 2SZ5 on the product distribution (CO free), toluene conversion, and PX selectivity in xylene. 10%# means that ZZO was directly deposited on Z5 powder. (**B**) Influence of Z5-modified times by TEOS on the product distribution (CO free), toluene conversion, and PX selectivity in xylene. (**C**) The comparisons of carbon usage and PX selectivity in xylene via methanol route and CO_2 route. (**D**) Apparent activation energy of toluene by methanol or CO_2/H_2 route on 4SZ5 or ZZO-4SZ5 catalysts, respectively. Reaction conditions: 360°C; 3.0 MPa; H_2/CO_2 = 3; gas hourly space velocity (GHSV) of mixture gas (CO_2 + H_2 + N_2) = 12,000 ml g^{-1} $hour^{-1}$; toluene vapored at 90°C [weight hourly space velocity (WHSV) of toluene = 1 $hour^{-1}$]; and time on stream, 15 hours. When using methanol: 3.0 MPa WHSV of toluene = 0.9 $hour^{-1}$; C_7H_8/CH_3OH = 6, GHSV of mixture gas (H_2 + N_2) = 12,000 ml g^{-1} $hour^{-1}$.

show that unmodified Z5 features a cube-like morphology and a clean surface. While Z5 was modified four times with TEOS and mixed with ZZO, zeolites show a tendency to become sphere, and small particles appear on the zeolite surface. Energy dispersive spectroscopy (EDS) line-scanning experiment indicates that the small particles are ZZO (Fig. 3, A to E). X-ray powder diffraction (XRD) pattern for ZZO shows a slight shift of ZrO_2 diffraction peaks to a high angle, suggesting that the small Zn atoms are successfully doped into the ZrO_2 crystal lattice to form ZZO solid solution structure (fig. S5A). Meanwhile, ZZO and Z5 are mixed at a mass ratio of 1:9, and the diffraction peaks of ZZO are difficult to recognize because the peaks of Z5 are too intense. The Brunauer-Emmett-Teller surface area of Z5 decreases from 360 to 253 m^2 g^{-1} as the number of modification times is increased. The decrement is mainly caused by the decrease of micropore area rather than external area based on the *t*-plot method (table S1). Meanwhile, pore size distribution curves show that the pore volume and the most probable pore size are reduced on the basis of the nonlocal density functional theory (NLDFT) (Fig. 3F) (*27*, *28*). This finding matches the result that 1,2,4-trimethylbenzen selectivity is decreased and 4-ethyltoluene selectivity is increased (Fig. 2A and fig. S1). The reductions in specific surface and pore size of Z5 after TEOS modification are essentially due to the changes of zeolite structure and crystallinity according to XRD results, although the molecular diameter of TEOS is larger than the pore size of intact Z5. Carbon dioxide temperature-programmed desorption (CO_2-TPD) curves indicate that CO_2 can be steadily adsorbed on ZZO until 550°C, but zeolites cannot adsorb CO_2 (fig. S5B). Acid amounts and types of zeolites are decisive for PX selectivity in xylene. Thus, ammonia TPD (NH_3-TPD) and pyridine Fourier transform infrared (Py-FTIR) spectroscopy are used to characterize acid properties. In the NH_3-TPD curves (Fig. 3G), three main peaks at 100° to 250°C, 250° to 550°C, and 550° to 700°C belong to weak acid, medium strong acid, and strong acid sites, respectively (*14*). Weak and medium strong acid are mainly contributed by zeolites, and strong acid is contributed by ZZO. The modified Z5 catalysts show an extreme decrease in the amount of medium acid compared with no modification. The more modified times performed, the less medium acid amount obtained. However, weak acid and strong acid amounts are changed slightly. In the Py-FTIR spectra shown in fig. S5C, the peaks at 1543, 1491, and 1448 cm^{-1} are attributed to pyridine adsorbed on Brønsted acid, surface hydroxyl, and Lewis acid sites, respectively. The quantity ratios of Brønsted acid to Lewis acid were calculated

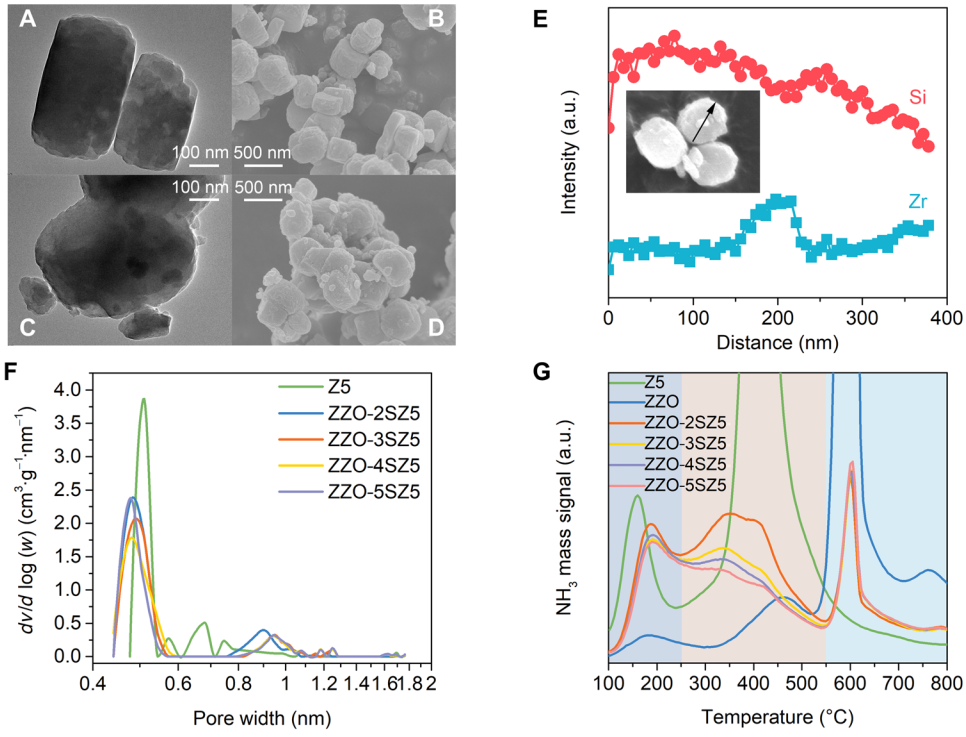

Fig. 3. Structural and acid characterizations of dual-functional catalysts. (**A**) TEM and (**B**) SEM images for Z5. (**C**) TEM, (**D**) SEM images, and (**E**) EDS line-scanning profiles for ZZO-4SZ5. a.u., arbitrary units. (**F**) Pore width distribution of Z5 and ZZO-Z5 series dual-functional catalysts based on the nonlocal density functional theory (NLDFT) method. (**G**) Ammonia TPD (NH_3-TPD) curves of Z5, ZZO, and ZZO-Z5 series dual-functional catalysts according to mass spectrometry signal.

from their corresponding peak intensities, which firstly rises up to 0.83 of ZZO-4SZ5 and then declines, with the number of zeolite-modified times increased. This result matches well with the tendency of PX selectivity in xylene (fig. S3), indicating that the higher Brønsted acid ratio of zeolite, the higher PX selectivity obtained. Al magic angle spinning nuclear magnetic resonance (MAS NMR) profiles show that all Al atoms in Z5 are tetra-coordinate at the zeolite framework. While Z5 is modified with TEOS, some lattice Al atoms are replaced by Si and converted to hexa-coordinate extra-framework octahedral aluminum (*29*, *30*). The signal-to-noise ratio of 4SZ5 is lower than that of Z5, which indicates that the content of Al decreases after zeolites are modified by TEOS (fig. S5D).

The H_2/D_2 kinetic isotope effect was obtained by fixed-bed reactor activity test to understand the reaction mechanism of toluene methylated with CO_2 and H_2 over ZZO-Z5 catalysts. While inletting D_2 instead of H_2 over ZZO-4SZ5 catalyst, toluene conversion increases from 14.5 to 18.2%, $k_H/k_D = 0.80$ (Fig. 4C). Such an inverse isotope effect indicates that the C—D bond is easier to form than the C—H bond, which may be related to the rate-determining step. Meanwhile, the outlet gas was injected into gas chromatography–mass spectrometer (GC-MS) to determine the substitution position by D atom. When the mixture of $H_2 + CO_2 + C_7H_8$ is used as the reactant, the mass spectra of toluene and xylene are consistent with the standard spectra, respectively (fig. S6). When H_2 is replaced by D_2, the mass-to-charge ratio (m/z) due to toluene moves from 91 to 95, indicating that H on benzene ring instead of methyl group can be readily substituted by D. For the mass spectrum of product taken from toluene methylated with CO_2 and D_2, the m/e main signal at 113 rather than 110 or 116 is observed, indicating the presence of a methyl group and a deuterated methyl group in xylene. Together, it can be concluded that the deuterated methyl group comes from the reduction of CO_2. The finding indicates that xylene is mainly derived from toluene methylation rather than disproportionation. In addition, H_2/D_2 and $CO_2/^{13}CO_2$ isotope-switching studies were performed using in situ diffuse reflectance infrared Fourier transform spectroscopy (in situ DRIFTS). All peak assignments are shown in table S2. When ZZO-4SZ5 is exposed to $CO_2 + H_2$, the species of HCOO* (1584 cm^{-1}) and slight CO_3* (1694 and 1525 cm^{-1}) are detected (fig. S7A) (*31*–*34*). When the catalyst is exposed to $C_7H_8 + CO_2 + H_2$, no any peak of CO_3* is observed (Fig. 4A), which means that the introduction of toluene would accelerate CO_2 hydrogenation rate by consuming intermediate species. When H_2 is switched to D_2, the peaks at 2166 and 2120 cm^{-1} appear, corresponding to the C—D asymmetric stretching and symmetric stretching vibrations for DCOO*, respectively. The peaks at 2709 and 2662 cm^{-1} are assigned to the O—D asymmetric stretching and symmetric stretching vibrations for OD*, respectively. The peaks at 3080 and 3035 cm^{-1} are assigned to the C—H stretching vibrations of benzene ring, and 2935 and 2884 cm^{-1} are assigned to the C—H stretching vibrations of the methyl group (*35*, *36*). In Fig. 4A, the peaks at 3080 and 3035 cm^{-1} decrease because of the replacement of H on benzene ring by D. Since the H on methyl group is unsubstituted, there is no decrease in the peak of 2935 and 2884 cm^{-1}, which is consistent with GC-MS results. The HCOO* (DCOO*) species increase after switching H_2 to D_2 in Fig. 4A and fig. S7A, indicating that the formation rate of DCOO* is higher than that of HCOO*, because of the different zero-point energy for isotope. For $CO_2/^{13}CO_2$ isotope-switching studies, when reaction gases are switched from $CO_2 + H_2 + C_7H_8$ to $^{13}CO_2 + H_2 + C_7H_8$,

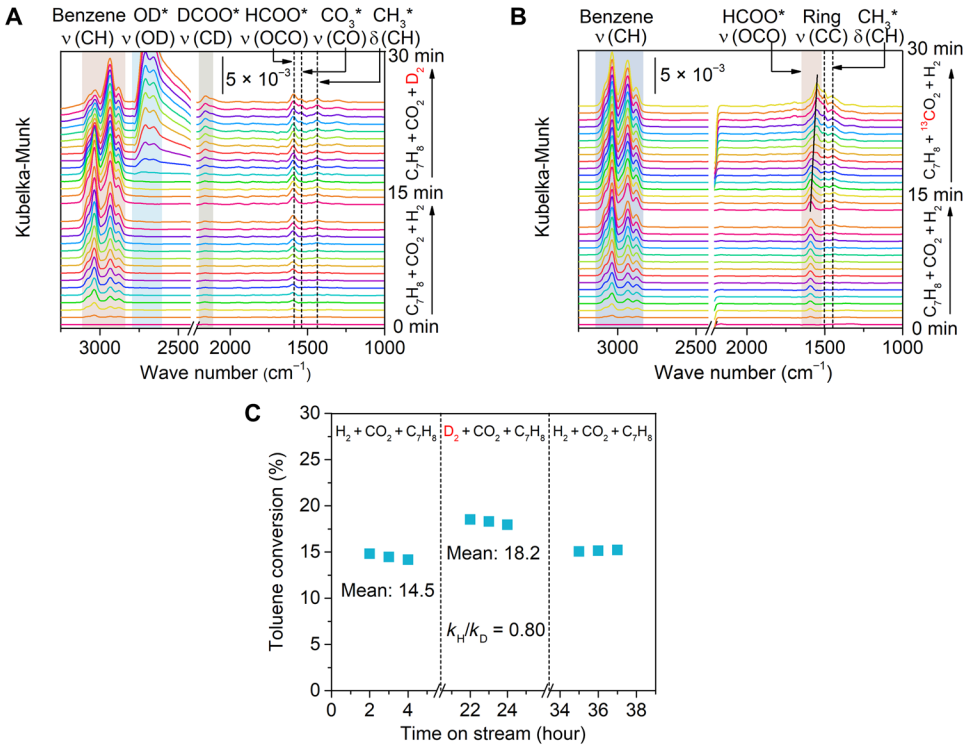

Fig. 4. H_2/D_2 or $CO_2/^{13}CO_2$ isotope effect studies. In situ DRIFTS spectra over the ZZO-4SZ5 catalyst exposed to the stream of (**A**) $C_7H_8 + CO_2 + H_2$ and subsequently switched to $C_7H_8 + CO_2 + D_2$ and of (**B**) $C_7H_8 + CO_2 + H_2$ and subsequently switched to $C_7H_8 + {}^{13}CO_2 + H_2$. (**C**) H_2/D_2 kinetic isotope effect of toluene methylated to xylene using CO_2 and $H_2(D_2)$ over ZZO-4SZ5 catalyst. Reaction conditions are the same as those in Fig. 2.

the O—C—O stretching vibration peak of HCOO* is shifted from 1584 to 1535 cm^{-1} (Fig. 4B). Meanwhile, the enhancement of the C—C stretching vibration of benzene ring (1503 cm^{-1}) and C—H bending vibration of CH_3* species (1437 cm^{-1}) indicates that more toluene is adsorbed on the catalysts, which may be because the slower rate of breaking ^{13}C—O than C—O bond reduces the methylation reaction rate. On the basis that HCOO* is the main species in DRIFTS, and the use of D_2 shows a higher reaction rate than H_2, the formation or hydrogenation of HCOO* is likely related to the rate-determining step. Combined with the DFT calculations in literature, the further hydrogenation of HCOO* to HCOOH* is suppressed by its reverse reaction, due to the high stability of HCOO*, which is consistent with in situ DRIFTS results above. The reverse reaction of HCOOH* to HCOO* is faster than not only HCOO* hydrogenation but also HCOOH* further hydrogenation (*37*–*39*). Thereby, we are more inclined to consider that the hydrogenation of HCOO* is the rate-determining step.

Reactive methylation species must migrate to the pore structure of zeolites to accomplish toluene methylation reaction. Therefore, the closer proximity of ZZO and zeolite, the higher U_{methy} could be obtained. To confirm the inference, different proximities of power-mixing, granule-mixing, and dual-bed mixed modes for ZZO and 4SZ5 were used, and the carbon usage of CO_2 was calculated. The power-mixing mode shows the highest U_{methy} up to 84.8%, whereas only 33.2% converted CO_2 participates in toluene methylation reaction under the dual-bed mode (Fig. 5A). The close proximity of the components in dual-functional catalysts could prominently accelerate the second step (toluene methylation) reaction rate in tandem reaction. With the consumption of reactive methylation species, the reaction equilibrium of CO_2 hydrogenation can be shifted to generate more reactive methylation species, which cause high U_{methy}. The stability test for ZZO-4SZ5 shows no obvious decline in toluene conversion and PX selectivity in xylene for more than 100 hours, but xylene selectivity decreases slightly and 4-ethyltoluene selectivity increases with time (Fig. 5B and fig. S8). Moreover, the catalyst that has been run for 100 hours is regenerated by a simple calcination in air and subjected to testing the performance to explore the reason of decrease in xylene selectivity. The results show that the xylene selectivity in initial stage is slightly lower than that over fresh catalyst, but it reaches to the same level after 40 hours on stream. The finding suggests that the decrease in xylene selectivity may not be caused by carbon deposition but is more likely that the changes of active and acidic sites of zeolite occurred in the process of reaction.

On the basis of the apprehension of toluene methylation using CO_2 and H_2 over ZZO-Z5 dual-functional catalysts, a possible reaction mechanism has been proposed as follows (Fig. 5C): (i) CO_2 is adsorbed on ZZO, and H_xCO* reactive methylation species are generated from CO_2 through the formate route. (ii) H_xCO* reactive species migrate onto the pore structure of Z5 with the hydrogenation of H_xCO* to H_3CO*. (iii) Toluene is adsorbed on H_3CO*, and xylene is produced through Friedel-Crafts methylation reactions in the channel of Z5. (iv) Xylene is desorbed from Z5, and a new active site is generated to finish a catalytic circle.

In conclusion, CO_2 and H_2 show great potential as methylation reagents for selectively methylating toluene to xylene over ZZO-Z5 dual-functional catalysts. Compared with methanol route, the reactive methylation species of H_3CO* entity is much easier obtained by the CO_2 hydrogenation route. Optimizing the mass ratio of ZZO

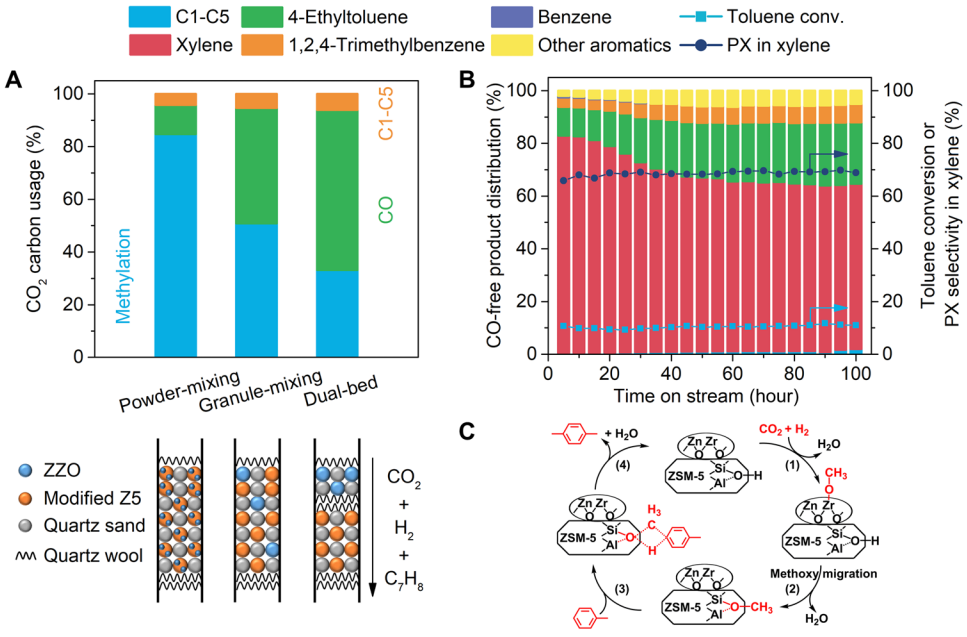

Fig. 5. The stability test and possible reaction mechanism. (**A**) Influence of different ZZO and 4SZ5 proximity on U_{methy}. Reaction conditions are the same as those in Fig. 2. (**B**) The stability test for ZZO-4SZ5 catalyst. (**C**) A possible reaction mechanism of toluene methylated with CO_2 and H_2 over ZZO-Z5 dual-functional catalyst.

to modified Z5 results in a high selectivity to xylene of 92.4% in CO-free products. Moreover, PX selectivity in xylene reaches to 70.8% over ZZO-4SZ5 in CO_2 route, while only 32.7% over 4SZ5 in methanol route. The reactive methylation species generated in CO_2 route is dynamically reacted by the subsequent methylation step, which substantially depressed the reactions of deep methylation and MTH. In the stability test of ZZO-4SZ5, toluene conversion and PX selectivity in xylene do not change significantly. CO_2 hydrogenation follows the formate route, and we tend to consider that the formation or hydrogenation of HCOO* is included in the rate-determining step. The proposed mechanism is that reactive methylation species are generated from ZZO by CO_2 hydrogenation and migrated to the pore structure of Z5 and methylating toluene to xylene. This work demonstrates the virtue of CO_2 hydrogenation coupled with toluene methylation over the dual-functional catalysts for PX production, which would inspire further explorations on other related systems.

MATERIALS AND METHODS

Catalyst preparation

ZZO was synthesized by a coprecipitation method based on the research of Li *et al.* (*14*). $Zn(NO_3)_2{\cdot}6H_2O$ (0.60 g) and $Zr(NO_3)_4{\cdot}5H_2O$ (5.80 g) were dissolved in 100 ml of deionized water labeled as solution A. $(NH_4)_2CO_3$ (3.06 g) was dispersed into 100 ml of deionized water labeled as solution B. Then, solution B was dropwise added into solution A at the speed of approximately 3 ml min^{-1} and continuously magnetically stirred for 2 hours at 70°C. After cooling down to ambient temperature and ageing for 2 hours, the precipitate was washed with deionized water, dried overnight, and calcined in air at 500°C for 3 hours. Z5 zeolites were purchased from the Nankai University Catalyst, and the method of using TEOS to modify Z5 was referred to the literature of Ni *et al.* (*16*). Typically, the steps to modify the Z5 once were to immerse 2.00 g of Z5 into the mix solution of 2.44 ml of TEOS and 1.00 ml of cyclohexane for 4 hours. Then, Z5 was dried at 110°C overnight and calcined in air at 550°C for 4 hours. While the above steps were repeated, a new symbol of *n*SZ5 (*n* means the number of repetitions) was used. Then, the dual-functional catalyst was obtained by the well mixing of ZZO and *n*SZ5 in an agate mortar. Before the performance in fixed-bed reactor system or the characterization of physicochemical properties, dual-functional catalysts were hydrogenated in 5% H_2/Ar mixed gas flow at 450°C for 2 hours.

Catalyst evaluation

Catalytic performance was evaluated on a high-pressure fixed-bed reactor equipped with a quartz sample tube. Typically, 200-mg catalyst (40 to 60 mesh) and 800-mg quartz sand were mixed and loaded into reaction tube. Before testing, samples were reduced by 5% H_2/Ar at 450°C for 2 hours. For the study of toluene methylated with CO_2 and H_2, a mixture gas of $CO_2/H_2/N_2$ [24/72/4 (v/v/v)] was induced into a stainless container loaded with toluene at 90°C, and then toluene was carried into reaction tube with a constant concentration. Typically, the reaction was conducted at 360°C and 3.0 MPa, with a GHSV of 12,000 ml g^{-1} $hour^{-1}$ and a toluene weight hourly space velocity (WHSV) of 1 $hour^{-1}$, and the data were collected at the reaction time of 15 hours. For the contrast experiment of toluene methylated with methanol, a mixed solution of C_7H_8/CH_3OH [2/1 (mol/mol)] was pumped into reaction tube with a toluene WHSV of 0.9 $hour^{-1}$ at 360° to 460°C and 0.1 and 3.0 MPa, while 12,000 ml g^{-1} $hour^{-1}$ N_2 or H_2/N_2 [72/28 (v/v)] was used as a carry gas simultaneously. Three GCs were used together equipped with PLOT-Q, WAX, and TDX-01 columns to analyze gaseous hydrocarbons, aromatics, and inorganic gases, respectively. CH_4 was taken as a reference bridge between the three GCs.

Toluene conversion was calculated according to

$$\mathrm{Conv}_{C_7H_8} = \frac{\sum_6^n \left(\frac{7}{n} C_n H_{m\mathrm{outlet}}\right) - C_7 H_{8\mathrm{outlet}}}{\sum_6^n \left(\frac{7}{n} C_n H_{m\mathrm{outlet}}\right)} \times 100\%$$

where $C_nH_{m\mathrm{outlet}}$ ($n \geq 6$) represents moles of aromatics at the outlet.

Product selectivity without CO for toluene methylated with CO_2 and H_2 was obtained according to

$$\mathrm{Sel}_{C_nH_m} = \frac{n C_n H_{m\mathrm{outlet}}}{\sum_1^n n C_n H_{m\mathrm{outlet}} - C_7 H_{8\mathrm{outlet}}} \times 100\%$$

where $C_nH_{m\mathrm{outlet}}$ ($n \geq 1$) represents moles of hydrocarbons at the outlet.

Product selectivity for toluene methylated with methanol was obtained according to

$$\mathrm{Sel}_{C_nH_m} = \frac{n C_n H_{m\mathrm{outlet}}}{\sum_1^n n C_n H_{m\mathrm{outlet}} - CH_3OH_{\mathrm{outlet}}} \times 100\%$$

where CH_3OH_{outlet} represents the mole of methanol at the outlet.

CO_2 carbon usages for methylation, C1-C5, and CO were obtained according to

$$U_{\mathrm{methy}} = \frac{\sum_6^n \left(\frac{n-7}{n} C_n H_{m\mathrm{outlet}}\right)}{\sum_6^n \left(\frac{n-7}{n} C_n H_{m\mathrm{outlet}}\right) + \sum_1^5 n C_n H_{m\mathrm{outlet}} + \mathrm{CO}_{\mathrm{outlet}}} \times 100\%$$

$$U_{C_1\text{–}C_5} = \frac{\sum_1^5 n C_n H_{m\mathrm{outlet}}}{\sum_6^n \left(\frac{n-7}{n} C_n H_{m\mathrm{outlet}}\right) + \sum_1^5 n C_n H_{m\mathrm{outlet}} + \mathrm{CO}_{\mathrm{outlet}}} \times 100\%$$

$$U_{\mathrm{CO}} = \frac{\mathrm{CO}_{\mathrm{outlet}}}{\sum_6^n \left(\frac{n-7}{n} C_n H_{m\mathrm{outlet}}\right) + \sum_1^5 n C_n H_{m\mathrm{outlet}} + \mathrm{CO}_{\mathrm{outlet}}} \times 100\%$$

where CO_{outlet} represents the mole of carbon monoxide at the outlet.

Methanol carbon usages for methylation, C1-C5, and DME were obtained according to

$$U_{\mathrm{methy}} = \frac{\sum_6^n \left(\frac{n-7}{n} C_n H_{m\mathrm{outlet}}\right)}{\sum_6^n \left(\frac{n-7}{n} C_n H_{m\mathrm{outlet}}\right) + \sum_1^5 n C_n H_{m\mathrm{outlet}} + 2\,CH_3OCH_{3\mathrm{outlet}}} \times 100\%$$

$$U_{C_1\text{–}C_5} = \frac{\sum_1^5 n C_n H_{m\mathrm{outlet}}}{\sum_6^n \left(\frac{n-7}{n} C_n H_{m\mathrm{outlet}}\right) + \sum_1^5 n C_n H_{m\mathrm{outlet}} + 2\,CH_3OCH_{3\mathrm{outlet}}} \times 100\%$$

$$U_{\mathrm{DME}} = \frac{2\,CH_3OCH_{3\mathrm{outlet}}}{\sum_6^n \left(\frac{n-7}{n} C_n H_{m\mathrm{outlet}}\right) + \sum_1^5 n C_n H_{m\mathrm{outlet}} + 2\,CH_3OCH_{3\mathrm{outlet}}} \times 100\%$$

where $CH_3OCH_{3\mathrm{outlet}}$ represents the mole of dimethyl ether at the outlet.

Catalyst characterization

XRD patterns were performed on a SmartLab SE diffractometer equipped with a Cu-K_α radiation source (λ = 1.5418 Å), operated at 40 kV and 40 mA, with a scan speed of 2°/min (2θ). Physical absorptions were carried out on a Micromeritics ASAP 2020 equipment. Initially, particle sample was degassed at 350°C under high vacuum for 3 hours to remove adsorbed moisture and organics. Then, measurements were executed, and Ar was used as adsorbate. Pore width distribution was obtained by NLDFT algorithm (*27*, *28*, *40*). NH_3-TPD and CO_2-TPD curves were carried out on a Micromeritics AutoChem 2920 apparatus with thermal conductivity detector, and a tandem online mass spectrum was used to monitor outlet gases. Typically, a pretreatment process by 5% H_2/Ar at 450°C for 1 hour over 50-mg catalysts was used before the above three types of temperature-programmed reactions. After the pretreatment process and cooling down to 50°C, 10% NH_3/Ar or pure CO_2 was inducted for 1 hour, and then the sample was exposed to Ar at 100°C for 2 hours until a stable baseline was obtained. Subsequently, the *m*/*z* signals of 16 for NH_3 and 44 for CO_2 were recorded by online mass spectrum, with the temperature increased to 800°C at a heating rate of 10°C/min. MAS NMR profiles were obtained on a Bruker AVANCE III equipment. Py-FTIR spectroscopy experiment was carried out on the same instrument as DRIFTS. A pretreatment process was carried out that the sample was exposed to 5% H_2/Ar at 450°C for 2 hours, and then inlet gas was changed into N_2, with the temperature returned to 80°C. After the temperature kept stably, inlet gas was turned off and vacuum pump was opened to vent the filled gas. Subsequently, the switch that is connected with pyridine was opened to induce pyridine volatilized into sample chamber for 3 min. Last, the entrance of pyridine was cut off, and gaseous or physical adsorbed pyridine was vacuumed, and then spectrums were recorded for 32 scans at the resolution ratio of 4 cm^{-1}. In situ DRIFTS measurements were performed on a Nicolet 6700 instrument equipped with a mercury cadmium telluride (MCT) detector at ambient pressure. First, the catalyst of ZZO-4SZ5 (ZZO mass percent, 50%) was exposed to 5% H_2/Ar at 450°C for 1 hour to obtain reduced state. Then, the inlet gas was changed into N_2 flow cooling down to 360°C, and a background was recorded. Toluene steam was induced by inletting reaction gases into a Monteggia washing bottle containing toluene at 80°C. All spectrums were obtained by collecting 32 scans at the resolution ratio of 8 cm^{-1}.

SUPPLEMENTARY MATERIALS

Supplementary material for this article is available at http://advances.sciencemag.org/cgi/content/full/6/34/eaba5433/DC1

REFERENCES AND NOTES

1. J. Zhou, Z. Liu, Y. Wang, D. Kong, Z. Xie, Shape selective catalysis in methylation of toluene: Development, challenges and perspectives. *Front. Chem. Sci. Eng.* **12**, 103–112 (2018).
2. J. H. Ahn, R. Kolvenbach, C. Neudeck, S. S. Al-Khattaf, A. Jentys, J. A. Lercher, Tailoring mesoscopically structured H-ZSM5 zeolites for toluene methylation. *J. Catal.* **311**, 271–280 (2014).
3. J. Zhou, Y. Wang, W. Zou, C. Wang, L. Li, Z. Liu, A. Zheng, D. Kong, W. Yang, Z. Xie, Mass transfer advantage of hierarchical zeolites promotes methanol converting into *para*-methyl group in toluene methylation. *Ind. Eng. Chem. Res.* **56**, 9310–9321 (2017).
4. J. H. Ahn, R. Kolvenbach, S. S. Al-Khattaf, A. Jentys, J. A. Lercher, Methanol usage in toluene methylation with medium and large pore zeolites. *ACS Catal.* **3**, 817–825 (2013).
5. Y. Bi, Y. Wang, Y. Wei, Y. He, Z. Yu, Z. Liu, L. Xu, Improved selectivity toward light olefins in the reaction of toluene with methanol over the modified HZSM-5 catalyst. *ChemCatChem* **6**, 713–718 (2014).
6. W. Tan, M. Liu, Y. Zhao, K. Hou, H. Wu, A. Zhang, H. Liu, Y. Wang, C. Song, X. Guo, Para-selective methylation of toluene with methanol over nano-sized ZSM-5 catalysts: Synergistic effects of surface modifications with SiO_2, P_2O_5 and MgO. *Micropor. Mesopor. Mater.* **196**, 18–30 (2014).
7. J. Zhang, W. Qian, C. Kong, F. Wei, Increasing *para*-xylene selectivity in making aromatics from methanol with a surface-modified Zn/P/ZSM-5 catalyst. *ACS Catal.* **5**, 2982–2988 (2015).
8. C. Wang, L. Zhang, X. Huang, Y. Zhu, G. Li, Q. Gu, J. Chen, L. Ma, X. Li, Q. He, J. Xu, Q. Sun, C. Song, M. Peng, J. Sun, D. Ma, Maximizing sinusoidal channels of HZSM-5 for high shape-selectivity to *p*-xylene. *Nat. Commun.* **10**, 4348 (2019).

9. J. H. Ahn, R. Kolvenbach, S. S. Al-Khattaf, A. Jentys, J. A. Lercher, Enhancing shape selectivity without loss of activity – Novel mesostructured ZSM5 catalysts for methylation of toluene to *p*-xylene. *Chem. Commun.* **49**, 10584–10586 (2013).
10. J. Li, H. Xiang, M. Liu, Q. Wang, Z. Zhu, Z. Hu, The deactivation mechanism of two typical shape-selective HZSM-5 catalysts for alkylation of toluene with methanol. *Cat. Sci. Technol.* **4**, 2639–2649 (2014).
11. S. Lee, D. Kim, J. Lee, Y. Choi, Y.-W. Suh, C. Lee, T. J. Kim, S. J. Lee, J. K. Lee, An *in situ* methylation of toluene using syngas over bifunctional mixture of Cr_2O_3/ZnO and HZSM-5. *Appl. Catal. Gen.* **466**, 90–97 (2013).
12. J. Wang, G. Li, Z. Li, C. Tang, Z. Feng, H. An, H. Liu, T. Liu, C. Li, A highly selective and stable ZnO-ZrO_2 solid solution catalyst for CO_2 hydrogenation to methanol. *Sci. Adv.* **3**, e1701290 (2017).
13. O. Martin, A. J. Martín, C. Mondelli, S. Mitchell, T. F. Segawa, R. Hauert, C. Drouilly, D. Curulla-Ferré, J. Pérez-Ramírez, Indium oxide as a superior catalyst for methanol synthesis by CO_2 hydrogenation. *Angew. Chem. Int. Ed.* **55**, 6261–6265 (2016).
14. Z. Li, Y. Qu, J. Wang, H. Liu, M. Li, S. Miao, C. Li, Highly selective conversion of carbon dioxide to aromatics over tandem catalysts. *Joule* **3**, 570–583 (2019).
15. X. Zhang, A. Zhang, X. Jiang, J. Zhu, J. Liu, J. Li, G. Zhang, C. Song, X. Guo, Utilization of CO_2 for aromatics production over ZnO/ZrO_2-ZSM-5 tandem catalyst. *J. CO2 Util.* **29**, 140–145 (2019).
16. Y. Ni, Z. Chen, Y. Fu, Y. Liu, W. Zhu, Z. Liu, Selective conversion of CO_2 and H_2 into aromatics. *Nat. Commun.* **9**, 3457 (2018).
17. Z. Li, J. Wang, Y. Qu, H. Liu, C. Tang, S. Miao, Z. Feng, H. An, C. Li, Highly selective conversion of carbon dioxide to lower olefins. *ACS Catal.* **7**, 8544–8548 (2017).
18. X. Liu, M. Wang, C. Zhou, W. Zhou, K. Cheng, J. Kang, Q. Zhang, W. Deng, Y. Wang, Selective transformation of carbon dioxide into lower olefins with a bifunctional catalyst composed of $ZnGa_2O_4$ and SAPO-34. *Chem. Commun.* **54**, 140–143 (2018).
19. N. Li, F. Jiao, X. Pan, Y. Chen, J. Feng, G. Li, X. Bao, High-quality gasoline directly from syngas by dual metal oxide–zeolite (OX-ZEO) catalysis. *Angew. Chem. Int. Ed. Engl.* **58**, 7400–7404 (2019).
20. K. Cheng, B. Gu, X. Liu, J. Kang, Q. Zhang, Y. Wang, Direct and highly selective conversion of synthesis gas into lower olefins: Design of a bifunctional catalyst combining methanol synthesis and carbon–carbon coupling. *Angew. Chem.* **128**, 4803–4806 (2016).
21. F. Jiao, J. Li, X. Pan, J. Xiao, H. Li, H. Ma, M. Wei, Y. Pan, Z. Zhou, M. Li, S. Miao, J. Li, Y. Zhu, D. Xiao, T. He, J. Yang, F. Qi, Q. Fu, X. Bao, Selective conversion of syngas to light olefins. *Science* **351**, 1065–1068 (2016).
22. Y. Wang, L. Tan, M. Tan, P. Zhang, Y. Fang, Y. Yoneyama, G. Yang, N. Tsubaki, Rationally designing bifunctional catalysts as an efficient strategy to boost CO_2 hydrogenation producing value-added aromatics. *ACS Catal.* **9**, 895–901 (2019).
23. A. Ramirez, A. Dutta Chowdhury, A. Dokania, P. Cnudde, M. Caglayan, I. Yarulina, E. Abou-Hamad, L. Gevers, S. Ould-Chikh, K. De Wispelaere, V. van Speybroeck, J. Gascon, Effect of zeolite topology and reactor configuration on the direct conversion of CO_2 to light olefins and aromatics. *ACS Catal.* **9**, 6320–6334 (2019).
24. A. Dokania, A. Ramirez, A. Bavykina, J. Gascon, Heterogeneous catalysis for the valorization of CO_2: Role of bifunctional processes in the production of chemicals. *ACS Energy Lett.* **4**, 167–176 (2019).
25. P. Zhang, L. Tan, G. Yang, N. Tsubaki, One-pass selective conversion of syngas to *para*-xylene. *Chem. Sci.* **8**, 7941–7946 (2017).
26. Y. Wang, W. Gao, S. Kazumi, H. Li, G. Yang, N. Tsubaki, Direct and oriented conversion of CO_2 into value-added aromatics. *Chemistry* **25**, 5149–5153 (2019).
27. P. Tarazona, Free-energy density functional for hard spheres. *Phys. Rev. A* **31**, 2672–2679 (1985).
28. P. Tarazona, U. M. B. Marconi, R. Evans, Phase equilibria of fluid interfaces and confined fluids. *Mol. Phys.* **60**, 573–595 (1987).
29. T. Blasco, A. Corma, J. Martínez-Triguero, Hydrothermal stabilization of ZSM-5 catalytic-cracking additives by phosphorus addition. *J. Catal.* **237**, 267–277 (2006).
30. P. Marturano, L. Drozdová, A. Kogelbauer, R. Prins, Fe/ZSM-5 prepared by sublimation of $FeCl_3$: The structure of the fe species as determined by IR, ^{27}Al MAS NMR, and EXAFS spectroscopy. *J. Catal.* **192**, 236–247 (2000).
31. C. Schild, A. Wokaun, A. Baiker, On the mechanism of CO and CO_2 hydrogenation reactions on zirconia-supported catalysts: A diffuse reflectance FTIR study: Part II. surface secies on copper/zirconia catalysts: Implications for methanoi synthesis selectivity. *J. Mol. Catal.* **63**, 243–254 (1990).
32. W. Li, K. Wang, J. Huang, X. Liu, D. Fu, J. Huang, Q. Li, G. Zhan, M_xO_y–ZrO_2 (M = Zn, Co, Cu) solid solutions derived from schiff base-bridged UiO-66 composites as high-performance catalysts for CO_2 hydrogenation. *ACS Appl. Mater. Interfaces* **11**, 33263–33272 (2019).
33. K. Chen, H. Fang, S. Wu, X. Liu, J. Zheng, S. Zhou, X. Duan, Y. Zhuang, S. C. E. Tsang, Y. Yuan, CO_2 hydrogenation to methanol over Cu catalysts supported on La-modified SBA-15: The crucial role of Cu–LaO_x interfaces. *Appl. Catal. Environ.* **251**, 119–129 (2019).
34. K. Chen, X. Duan, H. Fang, X. Liang, Y. Yuan, Selective hydrogenation of CO_2 to methanol catalyzed by Cu supported on rod-like $La_2O_2CO_3$. *Cat. Sci. Technol.* **8**, 1062–1069 (2018).
35. G. Muller, T. Narbeshuber, G. Mirth, J. A. Lercher, Infrared microscopic study of sorption and diffusion of toluene in ZSM-5. *J. Phys. Chem.* **98**, 7436–7439 (1994).
36. O. I. El-Sabbagh, M. M. Baraka, S. M. Ibrahim, C. Pannecouque, G. Andrei, R. Snoeck, J. Balzarini, A. A. Rashad, Synthesis and antiviral activity of new pyrazole and thiazole derivatives. *Eur. J. Med. Chem.* **44**, 3746–3753 (2009).
37. M. Dou, M. Zhang, Y. Chen, Y. Yu, DFT study of In_2O_3-catalyzed methanol synthesis from CO_2 and CO hydrogenation on the defective site. *New J. Chem.* **42**, 3293–3300 (2018).
38. M. Dou, M. Zhang, Y. Chen, Y. Yu, Theoretical study of methanol synthesis from CO_2 and CO hydrogenation on the surface of ZrO_2 supported In_2O_3 catalyst. *Surf. Sci.* **672–673**, 7–12 (2018).
39. S. Kattel, B. Yan, Y. Yang, J. G. Chen, P. Liu, Optimizing binding energies of key intermediates for CO_2 hydrogenation to methanol over oxide-supported copper. *J. Am. Chem. Soc.* **138**, 12440–12450 (2016).
40. A. S. Al-Dughaither, H. de Lasa, HZSM-5 zeolites with different SiO_2/Al_2O_3 ratios. Characterization and NH_3 desorption kinetics. *Ind. Eng. Chem. Res.* **53**, 15303–15316 (2014).

Acknowledgments

Funding: This work was supported by the National Key Research and Development Program of China (2017YFA0206801), the National Natural Science Foundation of China (21972113), and the Program for Innovative Research Team in Chinese Universities (IRT_14R31). **Author contributions:** J.Z. developed the sample synthesis approach and performed most of the experiments. W.C. provided help in the TEM measurements. J.L. helped to carry out the experiments in early stage. X.D. and L.Y. helped to analyze the data. J.Z. and Y.Y. wrote the manuscript. Y.Y. designed and guided the work. All the authors read and commented on the manuscript. **Competing interests:** Y.Y., J.Z., X.D., and L.Y. are the authors on a patent application related to this work (no. 201911149539.2, filed 21 November 2019). Y.Y., J.Z., X.D., and L.Y. are the authors on a second patent application related to this work (no. PCT/CN2020/077412, filed 2 March 2019). The other authors declare no conflict of interest. **Data and materials availability:** All data needed to evaluate the conclusions in the paper are present in the paper and/or the Supplementary Materials. The primary data that support the plots within this paper and other finding of this study are available from the corresponding author on reasonable request.

Submitted 15 December 2019
Accepted 9 July 2020
Published 21 August 2020
10.1126/sciadv.aba5433

Citation: J. Zuo, W. Chen, J. Liu, X. Duan, L. Ye, Y. Yuan, Selective methylation of toluene using CO_2 and H_2 to *para*-xylene. *Sci. Adv.* **6**, eaba5433 (2020).

Science Advances

Selective methylation of toluene using CO_2 and H_2 to *para*-xylene

Jiachang Zuo, Weikun Chen, Jia Liu, Xinping Duan, Linmin Ye and Youzhu Yuan

Sci Adv **6** (34), eaba5433.
DOI: 10.1126/sciadv.aba5433